Enzyme-linked immunosorbent assay using thin-layered microfluidics with perfect capture of the target protein

Journal:	*Analytical Methods*
Manuscript ID	AY-ART-10-2022-001686.R1
Article Type:	Paper
Date Submitted by the Author:	16-Dec-2022
Complete List of Authors:	Smirnova, Adelina; The University of Tokyo, School of Engineering Ohta, Ryoichi; The University of Tokyo, School of Engineering Mori, Emi; The University of Tokyo, School of Engineering Shimizu, Hisashi; The University of Tokyo, School of Engineering Morikawa, Kyojiro; The University of Tokyo, School of Engineering Kitamori, Takehiko; The University of Tokyo, School of Engineering

SCHOLARONE™
Manuscripts

ARTICLE

Enzyme-linked immunosorbent assay using thin-layered microfluidics with perfect capture of the target protein

Adelina Smirnova,[a] Ryoichi Ohta,[a] Emi Mori,[b] Hisashi Shimizu,[a] Kyojiro Morikawa,[a,c] and Takehiko Kitamori[a,c,d,*]

We developed a process for enzyme-linked immunosorbent assay on a glass microchip via the use of a thin-layered microfluidic channel. This channel possesses a high aspect ratio (width/depth ~200) and has an antibody layer immobilized directly on the channel surface. A depth of several microns and an excessive width and length (mm scale) of the channel provide a large-volume capacity (10^2 nL) and maximum capture efficiency of the analyte for a high level of detection sensitivity (10^2 pg mL^{-1}). The developed reusable immunosensor has demonstrated high-performance characteristics by requiring less than 50 μL of sample and providing analysis in less than 25 min. This new method could impact the development of point-of-care devices for biomedical applications.

Introduction

Compact and ultra-sensitive microfabricated devices with various integrated chemical processes (sampling, mixing, reaction, detection) and fast response is an oft-discussed topic for microfluidic applications, and has encouraged their active development in recent years.[1] Microfluidic devices provide highly efficient and fast reactions in a small space due to the fast diffusion rate provided by a high surface-to-volume ratio (S/V) and reductions in the consumption of reagent. Therefore, the cost of analysis is lowered when using this integrated and automated process, and sample handling is significantly simplified. Enzyme-linked immunosorbent assay (ELISA) is one of the most widely used techniques in biomolecule analysis for clinical diagnosis. ELISA can be applied for the detection of proteins, DNA, viruses, and cells. The recent demand for rapid point-of-care testing has grown extensively and ELISA on microfluidic devices is one of the solutions.[2]

Several techniques have been applied to implementing immunosorbent assay using microfabricated devices.[3–5] The devices themselves can be fabricated on different substrates such as silicon, glass, metals, polymers, and papers.[6] To bind antibodies, functionalized magnetic, polystyrene or latex beads, microspheres and particles have been utilized.[7] Beads-based microfluidic ELISA has already been commercialized and shown high levels of sensitivity (~ng mL^{-1}) and rapid (dozen of min) quantification characteristics for the detection of various immunoglobulins, antigens, and peptides.[8] However, the packing and removing of beads requires complicated fluidic operations. Using smaller diameter beads can often cause problems in the assay. The most critical one is an increase of back-pressure at the solution introduction procedure. Besides, dealing with air bubbles, which accidentally contaminated the packed bead region, is also very difficult in the case of smaller beads.[9] All these factors have motivated scientists to look for an alternative format for microfluidic ELISA without beads. Microfluidic paper-based analytical devices (μPADs) have

a. Collaborative Research Organization for Micro and Nano Multifunctional Devices, The University of Tokyo, 7-3-1, Hongo, Bunkyo, Tokyo 113-8656, Japan. E-mail: kitamori@icl.t.u-tokyo.ac.jp
b. Department of Applied Chemistry, School of Engineering, The University of Tokyo, 7-3-1, Hongo, Bunkyo, Tokyo 113-8656, Japan
c. Institute of Nanoengineering and Microsystems, Department of Power Mechanical Engineering, National Tsing Hua University, No. 101, Section 2, Kuang-Fu Road, Hsinchu 300044, Taiwan, R.O.C.
d. Department of Biomedical Engineering, Faculty of Engineering, Lund University, Lund 221 00, Sweden.

received much recent attention due to improvements in ease of use, but sensitivity is the main limiting factor.[10]

Devices with antibodies immobilized directly on the surface experience critical issues in controlling the surface properties.[11] Most of these devices are used in capillary-based microfluidics,[12,13] and chip-based versions have also been developed.[14,15] Typically, microchip-based methods use a 3-dimensional hydrogel co-polymerized with antibody-immobilized solid supports.[16,17] This method achieves a high S/V ratio inside the hydrogel and is easy to operate. With the chip-based method, however, the increase in the S/V ratio has attendant limitations on the sizes of channels and structures, which sometimes leads to the escape of an analyte protein. On the other hand, in 2014, our group pioneered a nanofluidic ELISA.[18] The nanofluidic format uses a nanospace of 10^2–10^3 nm width/depth with antibodies immobilized directly on the surface, which enables detection without beads due to an ultra-high S/V (10^6 m^{-1}) reaction field. The supremacy of the nanofluidic ELISA allows target antigens to be captured quickly (<1 min) and efficiently (close to 100%), which provides a new method for the counting of single molecules without the need for calibration.[19] This is a powerful tool for use in single-cell proteomics,[20–22] but these devices are difficult to apply to the processing of clinical sample volumes (nL~μL) due to the ultra-small size of nanochannels (fL).

Therefore, in order to meet the demand for onsite clinical utility, we developed a repeatable thin-layered ELISA[23] that provides input comparable to that of beads-based ELISA while maintaining the highly efficient capture level of nanofluidic ELISA. Based on the nanofluidic ELISA format, the channel width and length were expanded 10^3- and 10^1-fold to become several microns and 10 mm, respectively, for an increase in volume. Unlike polymer material, glass is a substrate that makes it possible to fabricate uniformed wide and long microfluidic channels with a depth of several microns. The channel depth was maintained as the S/V ratio of the reaction field, which is determined by the channel depth rather than by the channel width. As a result, a reaction field with a high S/V ratio (10^5–10^6 m^{-1}) and a large-volume capacity (100 nL) was achieved without using beads. As a target protein, we chose the well-known acute-phase C-reactive protein (CRP) that the liver produces in response to infection and inflammation. This protein has a well-

established ELISA protocol for its detection, for which we used a non-competitive sandwich mode of immunoassay. In previous work[23] we studied the proof-of-concept established for thin-layered ELISA and confirmed a fluidic control in the introduction of the sample. Also, we verified the working principle of thin-layered ELISA by measuring a standard CRP solution and evaluated the detection performance. In that previous work, however, we could not attain the maximum capture efficiency of the analyte, and, as a result, sensitivity remained relatively low (10^2 ng mL^{-1}).

In the present paper, we present the results of a thin-layered ELISA protocol that controls the channel depth, timing, and reagent concentration to achieve a capture efficiency of analyte that actually close to 100%. In addition, we were able to observe the analytical performance of CRP detection in both standard samples and in human serum.

Experimental

Reagents and materials

Reagents for surface modification

The (3-Aminopropyl) triethoxysilane (APTES) and ethanolamine were purchased from Sigma Aldrich (St Louis, MO, USA). Glutaraldehyde was purchased from Fujifilm-Wako Pure Chemical, Co. Ltd (Tokyo, Japan). Silanepolyethylene-glycol (PEG, molecular weight = 5000) was purchased from Nanocs (New York, NY, USA).

Reagents for analysis

Bovine serum albumin (BSA) was purchased from Johnson and Johnson (New Brunswick, NJ, USA). CRP and anti-CRP mouse IgG were purchased from Oriental Yeast, Co. Ltd (Tokyo, Japan) and used as an analyte protein and for the capture of antibodies, respectively. Horseradish peroxidase (HRP)-conjugated anti-CRP monoclonal antibody was purchased from Abcam (Cambridge, UK) and used as an enzyme-labeled or detection antibody. PBS (Phosphate Buffered Salts) tablets were purchased from Takara Bio Inc. (Kusatsu, Japan). A premixed solution of 3,3′,5,5′-tetramethylbenzidine and hydroperoxide solution (TMB) was purchased from Seracare Life Sciences, Inc. (Milford, MA, USA) and used as a substrate solution. Pool serum for accurate control of L-Consera was purchased from Nissui Pharmaceutical Co., LTD. Glycine, Tween

20, and Xylene Cyanol were purchased from Fujifilm-Wako Pure Chemical, Co. Ltd. (Tokyo, Japan). All reagents and solvents were of analytical grades or better. All solutions used for injection to the microchip were filtered via disposable membrane filter units (0.20 μm pore size).

Borosilicate substrates with thin-layered microfluidic ELISA channels were purchased from the Institute of Microchemical Technologies, Co., Ltd (Kawasaki, Kanagawa, Japan). A Simport microtube was used as a reservoir to deliver solutions to the microchip (2 mL volume).

Preparation of the thin-layered ELISA microchip

Our group developed a surface modification procedure[18] for bonding of the substrates via a low-temperature process.[24] Briefly, after plasma activation, we used Vacuum deposition of the APTES[25] on the surface of one substrate and plasma activation with Teflon species for another substrate. Following partial Vacuum-UV decomposition (through a mask) to remove the APTES from the glass — with the exception of the area comprising the thin-layered channel — the surface was washed with water and dried. Then both substrates were aligned and bonded at a low temperature of 110 °C for 3 hours.

After the microchip bonding and before the immobilization of antibodies, the channel was treated with silane-PEG after flushing with a 1.0 mg/mL^{-1} ethanol solution for 1.5 h to prevent the non-specific adsorption of other proteins. Then, antibodies were immobilized on the channel surface via a previously reported procedure.[18] Briefly, the remaining APTES was first bridged with bifunctional cross-linker glutaraldehyde by flowing a 2.5% solution in a borate buffer, pH 7.0, for 1.5 h. Then, the captured antibodies (25 μg mL^{-1} solution in PBS buffer) were linked for 1 h. Unreacted sites were quenched by flowing 0.5 M of ethanolamine/PBS for 10 min. The channel surface was then blocked with BSA by flowing a 2.0% BSA/PBS solution for 30 min. A schematic of the surface treatment of the thin-layered channel appears in **Scheme 1**.

Experimental setup and characterization of the thin-layered channel

The microchip was placed in a microchip holder. The two inlet holes on each side of the thin-layered channel were connected to reagent reservoirs, pressure controllers (MFCS-EZ, Fluigent,

Paris, France), and to an air compressor using capillaries (i.d. 0.26 o.d. 0.5 mm ICT-55P, Institute of Microchemical Technologies, Tokyo, Japan), Teflon connectors (UF-C, Institute of Microchemical Technologies, Tokyo, Japan), and o-rings (AS001, Air Water Mach, Inc., Nagano, Japan). The liquid flow inside the channel was controlled by applied pressure. For the ELISA readout, we used an Eclipse 80i microscope (Nikon Corporation, Japan) equipped with our original differential interference contrast thermal lens microscope (DIC-TLM).[26] Briefly, TLM is a kind of photo-thermal spectroscopy that measures absorption and nonradiative thermal relaxation. It is based on a probe laser beam refraction in thermal lenses formed in a microchannel due to an excitation beam absorption.[27] DIC-TLM use the probe beam polarization and splitting to realize background-free photo-detection in a liquid, so the S/N ratio can be improved by 1 order of magnitude compared to conventional TLM.[28] The sensitivity of the DIC-TLM is high enough to detect individual molecules in very short light pass distances, such as microfluidic channels with several microns or hundreds of nanometers depth.[26] To optimize the optical adjustments of DIC-TLM detection for absorbance maximization, and to control the flow parameters we used 0.1M Xylene Cyanol dye dissolved in washing buffer (0.2% BSA, 0.05% Tween 20 in PBS pH 7.4).

Thin-layered ELISA is a heterogeneous type of immunoassay in which antibodies are immobilized directly on the glass surface of a microfluidic channel to form a thin layer (the ideal case is a single molecule layer) of antibodies on a designated area. **Scheme 2** uses the TL-ELISA principle that is based on the use of a shallow microfluidic channel with a high S/V ratio and a single layer of immobilized antibodies. The captured antibodies were chemically conjugated to the glass surface with Si-O-H groups (activated by oxygen plasma) via a 3-aminopropyltriethoxysilane linker (APTES) and a glutaraldehyde (GA) bridge.

Vapor vacuum deposition of APTES creates a uniform coating on glass surfaces with a single layer of organosilane coupling agent.[25] The excess amino silane was easily removed from the surface via UV decomposition, which later allowed us to firmly bond two glass substrates at low temperature without interference. After the bonding, the channel surface area without APTES polymer was covered by non-adhesive poly-

(ethylene glycol) (PEG) chains via solvent deposition to prevent the non-specific adsorption of other proteins and biomolecules. Afterwards, the capture antibody was conjugated on the APTES area via GA (**Scheme 1**). Chemical adsorption of an antibody has an advantage over physical, because it allows the subsequent use of the same layer of antibody after recovery while Beads-ELISA requires washing away and the reintroduction of fresh beads. After the primary antibody is conjugated on the channel surface, a "sandwich" immunoassay procedure can be performed on the microfluidic chip, which includes the following sequential steps: analyte (CRP) and secondary antibody delivery (HRP), incubation, the washing of unbound antibodies, substrate delivery and enzymatic reaction (TMB), and detection (DIC-TLM).

The dimensions of our thin-layered microfluidic channel of 5.2 μm provided a surface-to-volume ratio (S/V) = 0.2 μm^{-1}, which is the same as that when using Beads-ELISA (45 μm), but without the need for beads. The S/V of the dry-etched rectangular glass channel directly depended on a channel depth of only 1/H. The shallower channel enhanced the capture efficiency. Nanochannels provide the highest efficiency.[19] For practical applications, however, we needed microfluidic channels in order to deal with samples at the nL~μL level. Even if capture efficiency depends solely on the depth of the channel, the area of capture for antibodies is responsible for the sensitivity of our immunosensor. In this work, we used two variations of TL-ELISA with the same surface area, but with different channel depths. Thin-layered channels of 2.0 and 5.2 μm in depth correspond to the S/V ratio of a Beads-ELISA microchip[29] (200 μm wide, 200 μm deep and 5 mm length) packed with beads with diameters of about 28 (packing density of 0.7) and 45 μm (packing density of 0.6), respectively. S/V was calculated as the surface area of the beads tightly packed in the microchannel to volume of the liquid between them.

Detection of CRP

The TL-ELISA protocol is presented in **Table 1**. All processes were performed at room temperature (23 °C). Constant fluid pressure was maintained at all times, except during the stopped flow of TMB for incubation and switching between reagents. The thin-layered channel was rinsed with a washing buffer

(0.2% BSA, 0.05% Tween 20 in PBS pH 7.4), and then a standard sample of CRP (200 nL of 1 – 500 ng mL^{-1}) was introduced for a limited time and immediately washed with the buffer by counter-flow. After changing the reagent, the channel was filled with enzyme-labeled antibody solution for the scheduled time and washed with the buffer. The secondary antibody solution was substituted by the substrate (TMB), which was introduced under high pressure, and flow was stopped for the 30 s needed for an enzymatic reaction. When the flow of TMB was resumed, the detection of the colorful product was performed downstream by DIC-TLM (excitation beam at 660 nm, 13 mW, probe beam at 532 nm, 1.5 mW). To recover the surface with immobilized primary antibody, the thin-layered channel was rinsed with Glycine Chloride (pH 2.5) and blocked by washing buffer (BSA) for 3 min.

Results and discussion

Characterization of the thin-layered channel

To maintain flow control and evaluate the flow velocity inside the microfluidic channels we used a colorful solution of Xylene.

Cyanol helped with estimating the filling rate via DIC-TLM signal change versus time. **Fig. 1** illustrates the signal change when the dye was delivered from the reservoir to the detection point (the entrance of the thin-layered channel).

The time when the signal reached maximum corresponded to the time when all buffer solutions in the connected capillary and channel were replaced by the dye (about 10 μL volume). We used this as the washing time when changing the reservoirs. We optimized the washing time by using 100 s for the long (CRP, HRP, buffer and Gly solutions delivery) channel and about 50 s for the short (TMB, buffer delivery) channel. The time before optimization was 5 min. Therefore, by simply reducing the connector's washing time we reduced the total analysis time from 45 to 23 min, which amounted to a reduction of almost half. We also used 0.1 mM of the Xylene Cyanol solution as a calibration standard to compare and adjust the results obtained on different days, since the optical settings and laser power can vary slightly from day to day.

Before running the actual ELISA measurements, we estimated the flow rate inside the TL channel by injecting Xylene

Please Analytical Methods argins

ARTICLE

Cyanol when one side of the connection channel was already filled with the dye solution, but the thin-layered channel was protected by the counter-flow of washing buffer due to the higher pressure in the other side of the connection channel. It normally takes 10 or 20 sec to completely replace the buffer solution with dye once the buffer flow is terminated, which corresponds to flow rates of 1.2 and 2 mm/s for 2.0- and 5.2−μm depth channels, with applied pressures of 250 and 100 kPa, respectively (**Fig. 2**).

This coincides with the data obtained in previous work for a channel with a depth of 5.2 μm.[23] The parameters of analyte injection were selected based on this data. Those parameters were 35 and 20 s for 2.0 and 5.2 μm depth channels, which corresponds to 0.08 and 0.2 μL of sample volume, respectively. The pressure resistance increased with a decrease in the channel cross-section, so we were forced to increase the applied pressure to ensure similar flow velocities. It should be noted that further decreasing the channel depth to 1 μm could result in such an increase in applied pressure to maintain a reasonable flow that it could exceed the pressure that a chip could withstand before collapsing due to low-temperature bonding. Thus, the range of the applied pressure is limited by the mechanical stability of the microchip and should not exceed 350 kPa.

Optimization of the experimental conditions

To attain a better sensing performance, we studied the influence of the secondary antibody concentration (HRP), reaction time, and flow rate on the immobilization process. Solutions with a constant CRP concentration of 0.02 μ g mL^{-1} were used for these measurements. The results appear in **Fig. 3**.

The signals increased with an increase in the concentration of HRP and reached a plateau at approximately 1.2 μ g mL^{-1}, and at the same point the background signal started to grow as well (**Fig. 3A**). The data are very similar to that from Beads-ELISA.[30] Time is another key factor in an immunoassay. And as **Fig. 3B** shows, an increase in the HRP injection time of from 60 to 120 s resulted in a more than twofold increase in the signal. However, pressure variations in the 5.2 μm channel showed insignificant influence on the reaction (**Fig. 3C**). For the 2.0 μm

chip, we had no room to vary the pressure due to a high level of flow resistance, and used only a single pressure of 250 kPa. These results prove that the limiting factor is not the rate of reagent delivery, but, rather, it is the kinetics near the surface of the sensor, where concentration and residence time are key factors. Therefore, we selected 1.5 μg mL^{-1} of HRP and 100 s of reaction time for further measurements of both the 2.0 and 5.2 μm channels on microfluidic chips. The previous unoptimized parameters were 0.1 μg mL^{-1} of HRP and 60 s of reaction time.[23]

To confirm efficient surface recovery and reproducibility of the assay, we measured the signal both with and without antigen (CRP) over several repetition cycles (**Fig. 4**). As shown in **Fig. 4**, the background signal was completely restored in the next cycle following every introduction of a high concentration of antigen (50 ng/mL). Therefore, we confirmed that the established surface recovery procedure of cleansing the channel surface of the immobilized antibody with glycine chloride (pH 2.5) and blocking with BSA (pH 7.4) is effective for a thin-layered ELISA assay. Also, the microfluidic chip is reusable, and the same antibody layer can be utilized for numerous tests.

Quantitative analysis of CRP

Under the optimized experimental conditions, different concentrations of CRP were added to evaluate the performance of the proposed microfluidic immunosensor. **Fig. 5 (A, B)** shows the specific signal peaks correlated with the concentrations of CRP. Thus, the working principle of thin-layered ELISA was again confirmed. Signal values were defined from the peak heights, a calibration curve was obtained by plotting signals against concentration, as shown in **Fig. 5C**. The detection limits (LoD) were estimated using the measurements of the standard deviation of a blank signal (3.3σ) and were 0.16 and 0.33 ng mL^{-1} for 2.0 and 5.2 μm, respectively. The relative standard deviation (RSD) was calculated for two consecutive experiments performed at a concentration of 5 ng mL^{-1} and showed similar values of 1.8 and 2.0%. Optimization of the immobilization conditions led to an increase in the sensitivity of the method, and, hence, to a decrease in the detection limit by two orders of magnitude from 34 ng mL^{-1} to below 0.4 ng mL^{-1}. Detection limits depends on the surface area of primary antibody, and if

increased the limits can be extended more. Also, precise optics adjustments of DIC-TLM can increase the signal and make an improvement.

Besides, the antibody layer stability itself influences on a performance of the assay and detection limits, and the storage conditions is essential to keep the stability high. The fabricated and immobilized TL-ELISA microfluidic chip was blocked by BSA, sealed with masking tape and stored at 4 °C for 4 weeks and then used for studies. Almost no difference in the absorbance signal was obtained either from the freshly made chip or following storage. This indicates that the TL-ELISA chip has good stability under proper storage conditions. However, there is a danger of the solution drying out in the microfluidic channels, and, as a consequence, there would be a decrease in the antibody activity. Therefore, it is advisable not to store the microchip under wet conditions for long periods of time. A longer shelf life requires the development of a new dry-storage technology, on which we are currently working.

Influence of the channel depth

To compare and choose between 2.0 and 5.2 μm depths for the microfluidic sensors, we needed to evaluate competing physical processes such as convection, diffusion, and reaction to determine how they drive molecular transport within the channels. Based on our experimental results, we estimated parameters (presented in **Table 2**) such as two Peclet numbers (Pe$_h$ and Pe$_s$) and a Damkohler number (Da) according to the calculations for surface-based biosensors.[31–33]

However, in our case the length of the sensor (L) was much longer than the depth of the channel (H), so the values for λ = L/H were 5,000 and 2,000 for 2.0 and 5.2 μm channels, respectively, which exceeds all previously calculated limits.[31–33] The Damkohler number, Da, involves the kinetic constant of the forward reaction rate, k$_{on}$, the surface concentration of the antibody, b$_m$ (the total number of the free sites available for binding, $10^2/\mu m^2$ [19]), the length of the sensor, and diffusivity, which combines the relative strength of the reaction at the surface and the diffusion towards it. In our case for both chips, Da was >>1 (10^{10}), which shows that the equilibrium is limited solely by the rate of sample diffusion to the sensor, rather than by the kinetic reaction. The first Peclet number, Pe$_s$, takes into

account volumetric flow, length, height, and width of the sensor, and depends upon shear rate and sensor length. The Pe$_s$ for our channels were also >>1 (10^9), and are characteristic of the thin depletion zone, δ=LPe$_s^{-1/3}$, which forms above the sensor and equates to 5.6 and 5.1 μm for 5.2 and 2.0 μm channels, respectively. To collect all antigens, the depletion zone must be thicker than the channel height, LPe$_s^{-1/3}$>>H. This means that a 5.2 μm channel depth would not meet the required standards, by comparison with a 2.0 μm channel. Another Peclet number, Pe$_h$, is the ratio of convection and diffusion strength with values of about 250 for 5.2 μm and 50 for 2.0 μm channels. This shows that convection prevails in the taller channel and diffusion dominates in the shallow channel. This observation is supported by experimental results, when the signals are similar for a different number of molecules due to different injection volumes of the same concentration (0.2 nL versus 0.063 nL in 5.2 and 2.0 μm channels, respectively). The collection rate, J$_D$[31], was lower in the taller channel due to the thin depletion zone and higher convection flux. We calculated the collection time, = N/J$_D$, where N represents injected molecules, and when C$_0$ = 50 ng mL^{-1} the collection required 18.0 and 6.3 s for 5.2 and 2.0 μm channels, respectively. Calculation for the reaction equilibrium time, t$_r$ = (k$_{off}$+k$_{on}$C$_0$)$^{-1}$, was about 15 sec for our sensor area. We used 20 and 35 sec for injection time at depths of 5.2 and 2.0 μm, which corresponds to the time sufficient to pass a volume of analyte solution approximately equal to double the volume of a thin-layered channel. However, calculations have shown **(Fig. 6)** that 20 s is insufficient to collect all injected molecules in a 5.2 μm channel. Therefore, the number of captured molecules in the tall channel (~55%) equaled that of the shallow channel (100% - grey zone in **Fig. 6**). As **Fig. 6** shows, both time and pressure are limiting factors. To ensure 100% capture efficiency the time must meet the following conditions: injection time > collection time > equilibrium time, while the pressure should not exceed 350 kPa to maintain the integrity of the chip. The red circles show the present experimental conditions and demonstrate that conditions on the 5.2 μm chip are far from 100% capture efficiency. That observation is supported by the experimental data that show the same signal for a different number of molecules (same concentrations but different injected volumes)

(**Fig. 3 – 5**). The signal intensity of DIC-TLM, as observed with the absorbance spectroscopic method, can be described by Beer's law, $A = \varepsilon l C$, where the concentration $C(CRP)$ depends on the number of molecules, N, of the captured antibody on the area, S, diluted to volume, $V=Sl$, where l is simultaneously the channel depth, H, and the length of the light path length. Because the 5.2 and 2.0 μm channels have an equal area, S, for the capture of antibodies, the signal intensity is not dependent on the l; it depends only on the number of captured antigens: $A = \varepsilon l(N/Sl) = \varepsilon N/S$. The results of **Figs. 4-6** confirm our assumptions that the signal, aka the number of captured antigens, is almost equal for the 5.2 and 2.0 μm channel depths despite the different volumes of solutions of the same concentration, which is due to the lower capture efficiency in the 5.2 μm channel.

To verify this assumption, we injected the same volume of the same concentration of the CRP solution (20 ng mL^{-1}) using different combinations of applied pressure and injection times (**Fig. 2**), and the results appear in **Fig. 7**. As expected, low flow velocities alone with longer injection times led to a signal increase and hence to an increase in capture efficiency, and reached a constant level with parameters from the purple oval zone shown in **Fig. 6**. Such signal saturation cannot be achieved due to either substrate depletion or depleting all available binding sites, because higher protein concentrations show much higher signals while using the same concentration of substrate and same number of binding sites. For example, on Fig. 4 we used higher concentrations of CRP for injection to confirm the surface recovery. New Peclet numbers, Pe$_h$, for these zones (29-33kPa) fell as low as 80-100, which made them comparable to the Pe$_h$ for the 2.0 μm channel (**Table 2**). We recalculated the depletion zone, $\delta=LPe_s^{-1/3}$, as well, and found it ranged from 7.6~8 μm, and started to meet the conditions where the depletion zone exceeded the channel depth of 5.2 μm ($\delta \gg H$). All these results show that at low-pressure injections, diffusion started to dominate the convection process to provide a maximum capture efficiency close to 100%.

Tests of real samples

To verify the applicability of the proposed sensor, we tested standard samples of human serum with known concentrations of CRP. The results of the reliability of the proposed sensors are presented in **Table 3**. For TL-ELISA measurements the standard samples of 3.7 and 20 μg mL^{-1} were diluted to match the calibration range of our assay (1 – 50 ng mL^{-1}) by 200 and 1,000 times, respectively. This method is highly sensitive and real samples need to be diluted by 10 to 1000 times to fit into the calibration range, so non-specific serum-based interferences and sample high viscosity can be overcome by dilution. Also, it is highly selective based on double specificity of a sandwich ELISA and gave no false positives from other interfering proteins, such as IL-6 (0.01-0.10 μg/mL) (data not shown). The results for 2.0 and 5.2 μm microfluidic channels showed no remarkable differences (Table 3). However, the 5.2 μm channel has a more controllable pressure flow and less risk of either channel clogging or mechanical failure of the device. Therefore, in further experiments, we prefer to work with 5.2 μm channels but with adjustments to the injection time and pressure to ensure maximum capture efficiency (parameters in the purple oval in **Fig. 7**). Also, we could fabricate a new channel with a 3~4 μm depth and evaluate the performance on such a new thin-layered ELISA microfluidic chip.

Conclusions

In summary, we developed a novel immunosensor based on a microfluidic chip with a thin layer of immobilized antibodies and maximized capture efficiency of the analyte. Along with highest capture efficiency, a high level of sensitivity (0.3 - 50 ng mL^{-1}) for the detection of CRP was achieved. The developed reusable immunosensor demonstrated high-performance characteristics, required less than 50 μL of a sample, and took less than 25 min for analysis and can compete with other point-of-care systems.[2] We demonstrated its application for the detection of CRP in human serum. Automation through integration with programmable pumps, valves, and injectors could lead to further ease of use, sample savings, and even shorter analysis times of ~10 min. When introduced in a portable device this method could be applied for the sensitive monitoring of C-reactive protein as a biomarker for inflammation in a small number of blood samples, which would

make a positive contribution to clinical diagnostics as a near-patient and point-of-care testing.

Conflicts of interest

There are no conflicts to declare

Acknowledgements

References

1   A. H. C. Ng, U. Uddayasankar and A. R. Wheeler, *Anal. Bioanal. Chem.*, 2010, **397**, 991–1007.

2   S. K. Vashist, A. G. Venkatesh, E. Marion Schneider, C. Beaudoin, P. B. Luppa and J. H. T. Luong, *Biotechnol. Adv.*, 2016, **34**, 272–290.

3   H. Shi, K. Nie, B. Dong, M. Long, H. Xu and Z. Liu, *Chem. Eng. J.*, 2019, **361**, 635–650.

4   M. Herrmann, E. Roy, T. Veres and M. Tabrizian, *Lab Chip*, 2007, **7**, 1546–1552.

5   J. Park, V. Sunkara, T. H. Kim, H. Hwang and Y. K. Cho, *Anal. Chem.*, 2012, **84**, 2133–2140.

6   L. Mou and X. Jiang, *Adv. Healthc. Mater.*, 2017, **6**, 1601403–1601423.

7   R. Khnouf, G. Goet, T. Baier and S. Hardt, *Analyst*, 2014, **139**, 4564–4571.

8   Example of Microchemical System, Institute of Microchemical Technology.

9   K. Sato, M. Yamanaka, T. Hagino, M. Tokeshi, H. Kimura and T. Kitamori, *Lab Chip*, 2004, **4**, 570–575.

10   C.-A. Chen, W.-S. Yeh, T.-T. Tsai, Y.-D. Li and C.-F. Chen, *Lab Chip*, 2019, **19**, 598–607.

11   Y. Bai, C. G. Koh, M. Boreman, Y.-J. Juang, I.-C. Tang, L. J. Lee and S.-T. Yang, *Langmuir*, 2006, **22**, 9458–9467.

12   T. G. Henares, E. Tsutsumi, H. Yoshimura, K. Kawamura, T. Yao and H. Hisamoto, *Sensors Actuators B Chem.*, 2010, **149**, 319–324.

13   W.-J. Kim, H. Cho, B. Jeong, S. Byun, J. Huh and Y. Kim, *Sensors*, 2018, **18**, 55–67.

14   T. Wang, M. Zhang, D. D. Dreher and Y. Zeng, *Lab Chip*, 2013, **13**, 4190–4197.

15   J. Horak, C. Dincer, H. Bakirci and G. Urban, *Biosens. Bioelectron.*, 2014, **58**, 186–192.

16   W. C. Sung, H. H. Chen, H. Makamba and S. H. Chen, *Anal. Chem.*, 2009, **81**, 7967–7973.

17   M. Ikami, A. Kawakami, M. Kakuta, Y. Okamoto, N. Kaji, M. Tokeshi and Y. Baba, *Lab Chip*, 2010, **10**, 3335–3340.

18   K. Shirai, K. Mawatari and T. Kitamori, *Small*, 2014, **10**, 1514–1522.

19   K. Shirai, K. Mawatari, R. Ohta, H. Shimizu and T. Kitamori, *Analyst*, 2018, **143**, 943–948.

20   T. Nakao, Y. Kazoe, E. Mori, K. Morikawa, T. Fukasawa, A. Yoshizaki and T. Kitamori, *Analyst*, 2019, **144**, 7200–7208.

21   L. Lin, K. Mawatari, K. Morikawa, Y. Pihosh, A. Yoshizaki and T. Kitamori, *Analyst*, 2017, **142**, 1689–1696.

22   K. Yamamoto, K. Morikawa, H. Shimizu, H. Sano, Y. Kazoe and T. Kitamori, *Lab Chip*, 2022, **22**, 1162–1170.

23   T. Nakao, K. Mawatari, Y. Kazoe, E. Mori, H. Shimizu and T. Kitamori, *Analyst*, 2019, **144**, 6625–6634.

24   R. Ohta, K. Mawatari, T. Takeuchi, K. Morikawa and T. Kitamori, *Biomicrofluidics*, 2019, **13**, 024104.

25   F. Zhang, K. Sautter, A. M. Larsen, D. A. Findley, R. C. Davis, H. Samha and M. R. Linford, *Langmuir*, 2010, **26**, 14648–14654.

26   H. Shimizu, K. Mawatari and T. Kitamori, *Anal. Chem.*, 2010, **82**, 7479–7484.

27   T. Kitamori, M. Tokeshi, A. Hibara and K. Sato, *Anal. Chem.*, 2004, **76**, 52 A-60 A.

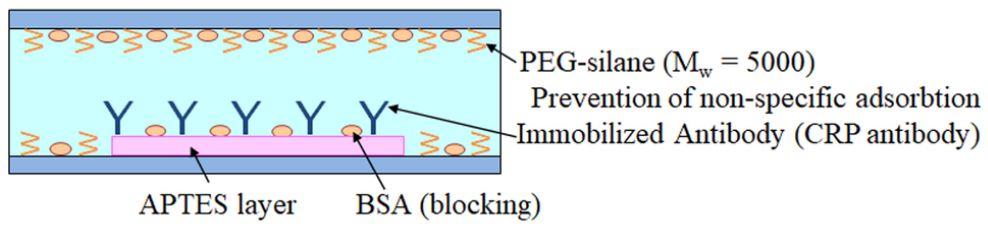28   H. Shimizu, K. Mawatari and T. Kitamori, *Anal. Chem.*, 2009, **81**, 9802–9806.

29   T. Ohashi, K. Mawatari, K. Sato, M. Tokeshi and T. Kitamori, *Lab Chip*, 2009, **9**, 991–995.

30   T. Ohashi, K. Mawatari and T. Kitamori, *Biomicrofluidics*, 2010, **4**, 032207-1-032207–7.

31   T. M. Squires, R. J. Messinger and S. R. Manalis, *Nat. Biotechnol.*, 2008, **26**, 417–426.

Journal Name

32   S. Jomeh and M. Hoorfar, *Chem. Eng. J.*, 2010, **165**, 668–
     677.

33   T. Gervais and K. F. Jensen, *Chem. Eng. Sci.*, 2006, **61**,
     1102–1121.

1
2
3
4
5
6
7
8
9
10
11
12
13
14
15
16
17
18
19
20
...
60

PEG-silane (M_w = 5000)
Prevention of non-specific adsorbtion
Immobilized Antibody (CRP antibody)

APTES layer   BSA (blocking)

Scheme 1. Chemical bonds on the surface of Thin-layered channel.

82x22mm (300 x 300 DPI)

1
2
3
4
5
6
7
8
9
10
11
12
13
14
15
16
17
18
19
20
21
22
23
24
25
26
27
28
29
30
31
32
33
34
35
36
37
38
39
40
41
42
43
44
45
46
47
48
49
50
51
52
53
54
55
56
57
58
59
60
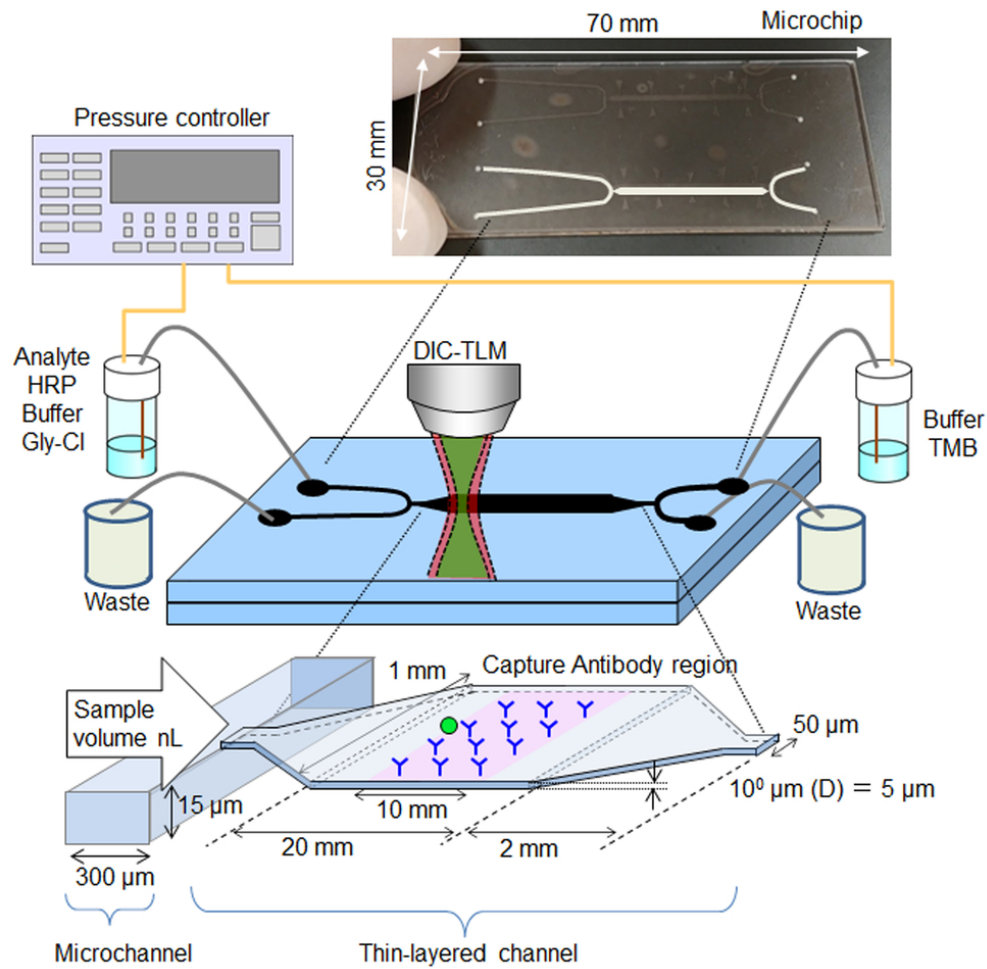
Scheme 2. The TL-ELISA microchip, an experimental setup and a close-up of microfluidic channels with immobilized antibody layer.

82x81mm (300 x 300 DPI)

1
2
3
4
5
6
7
8
9
10
11
12
13
14
15
16
17
18
19
20
21
22
23
24
25
26
27
28
29
30
31
32
33
34
35
36
37
38
39
40
41
42
43
44
45
46
47
48
49
50
51
52
53
54
55
56
57
58
59
60
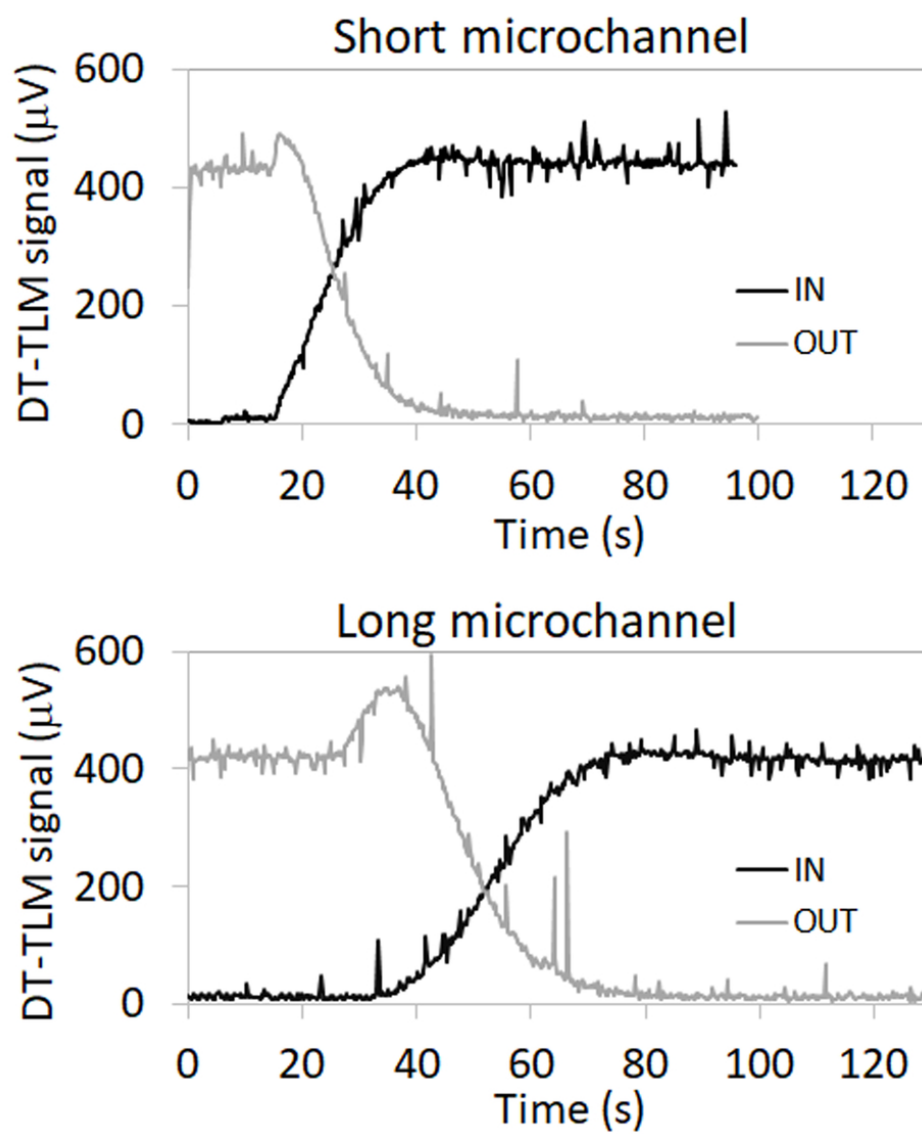
Fig. 1 Optimization of time of washing microfluidic channels with Xylene Cyanol 0.1 mM.

82x95mm (300 x 300 DPI)

1
2
3
4
5
6
7
8
9
10
11
12
13
14
15
16
17
18
19
20
21
22
23
24
25
26
27
28
29
30
31
32
33
34
35
36
37
38
39
40
41
42
43
44
45
46
47
48
49
50
51
52
53
54
55
56
57
58
59
60
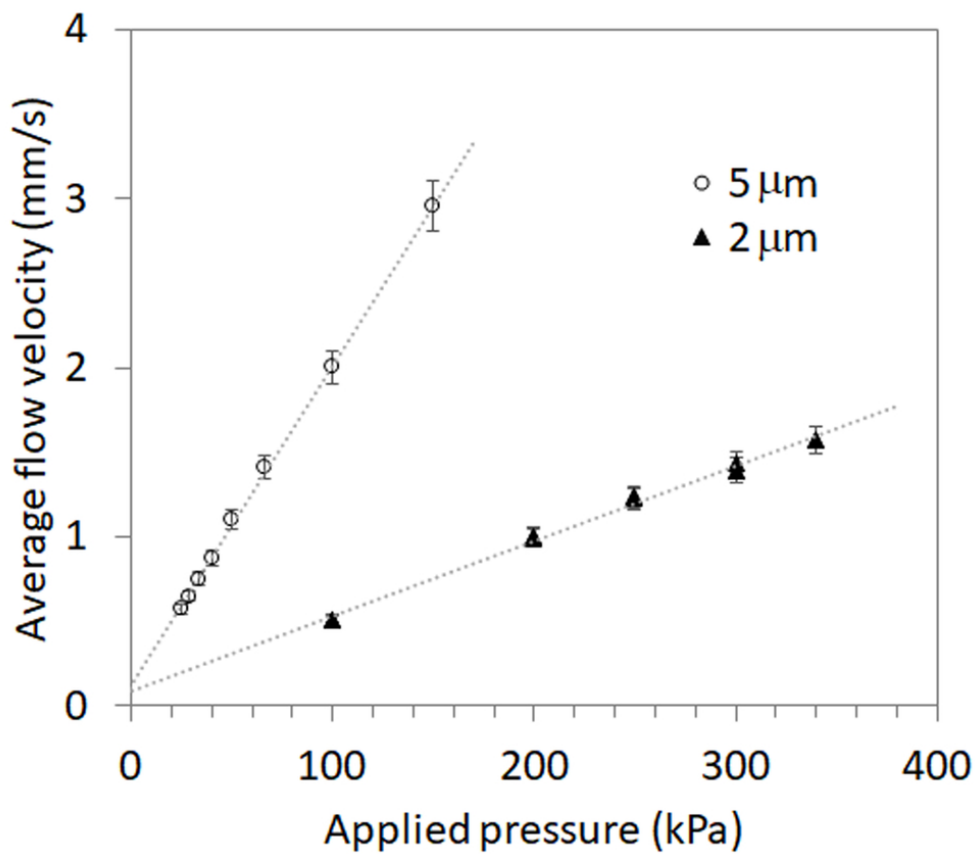
Fig. 2. Average flow velocity in thin-layered channel plotted against the applied pressure.

82x72mm (300 x 300 DPI)
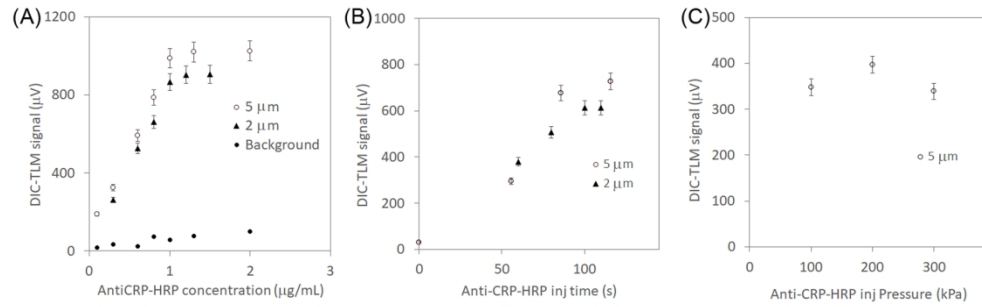
Fig. 3. Optimization of immobilization conditions: the effect of secondary antibody concentration (A), reaction time (B) and applied pressure (C). The concentration of CRP = 20 ng/mL (A,B,C), the concentration of HRP = 0.6 µg/mL (B, C), HRP residence time 60s (C).

170x53mm (300 x 300 DPI)
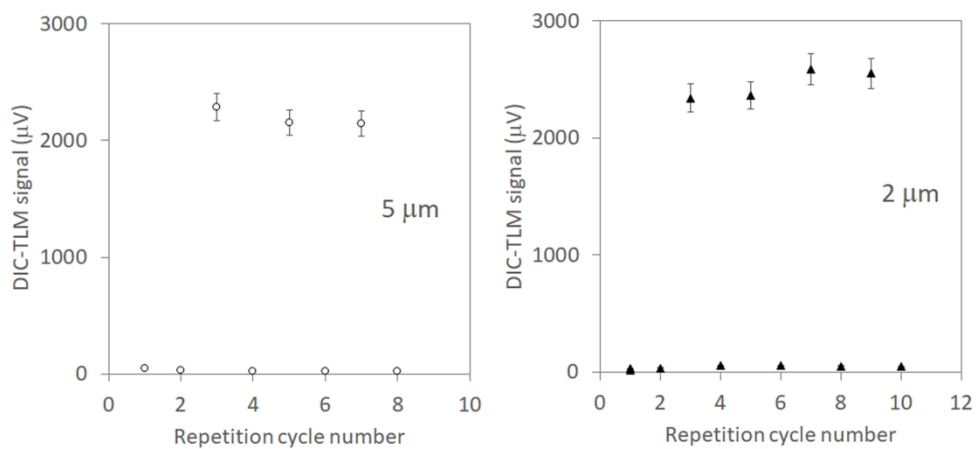
Fig. 4. Surface recovery cycles using Glycine Chloride buffer (pH 2.5) for 2 and 5.2 µm channel depth TL-ELISA.

165x78mm (300 x 300 DPI)
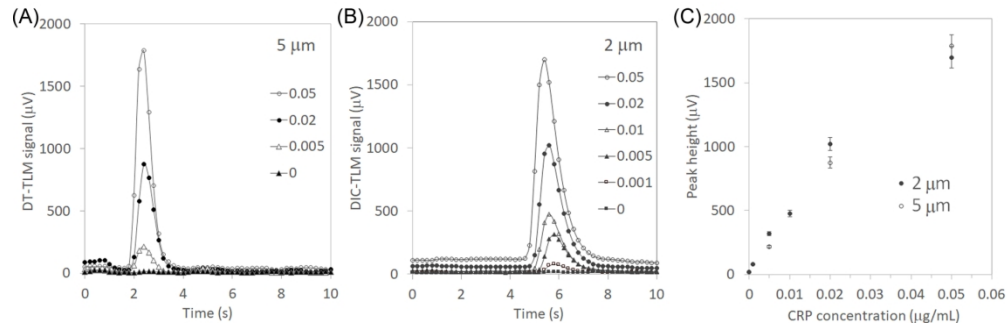
Fig. 5. Concentration dependences and standard curves for 2 and 5.2 μm channel depth TL-ELISA.

170x54mm (300 x 300 DPI)
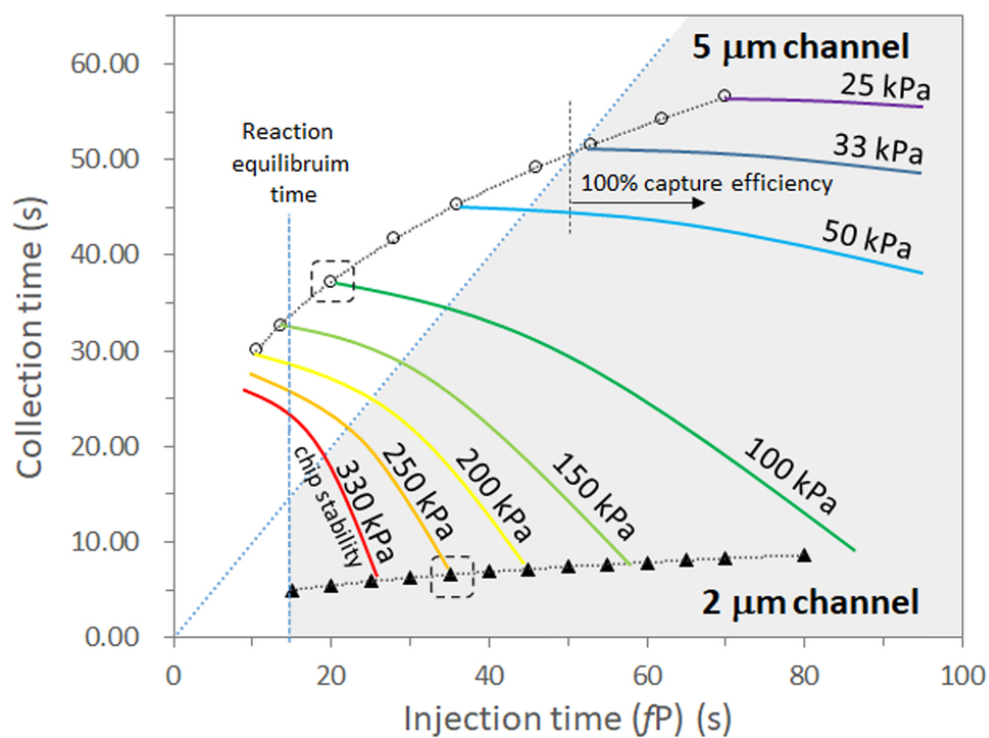
Fig. 6. Calculations of dependency of injection time (function of pressure to fill thin-layered channel, Fig. 2) on the collection time (also depends on the volumetric flow). Dashed square – present parameters used for the experiments, 100% capture efficiency line – recommended parameters for 5.2 µm channel, grey zone – 100% capture efficiency ($t_{injection} > t_{collection} > t_{equilibrium}$).

82x62mm (300 x 300 DPI)
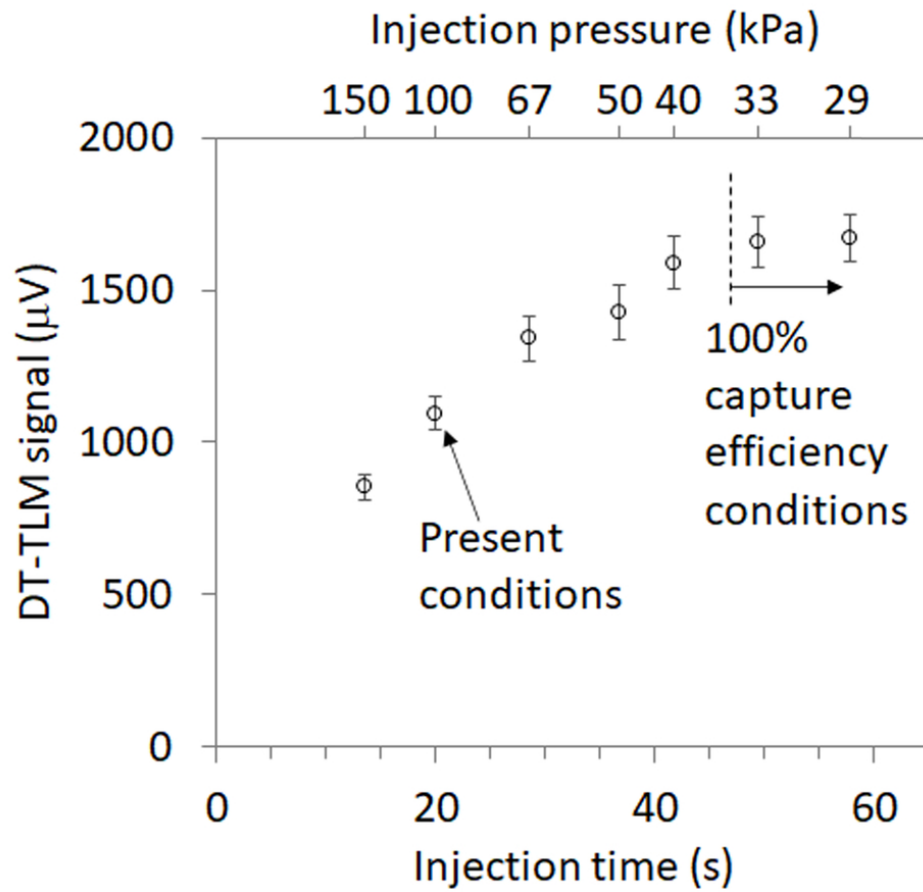
Fig. 7. The influence of the injection time as the function of the applied pressure on the immunosensor's performance (5.2 μm depth thin-layered channel). Red circle marks present injection conditions, purple oval marks 100% capture efficiency conditions.

82x76mm (300 x 300 DPI)

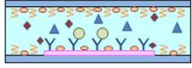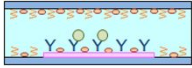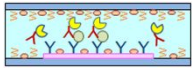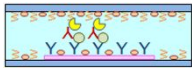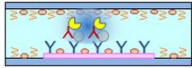*Table 1.   Typical protocol for TL-ELISA: timing, approximate volume*
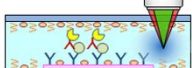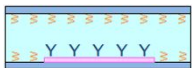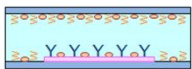
Step	Reagent	Washing step			Injection (5.2µm channel / 2.0 µm channel)			Schematic illustration
		Time [s]	Volume (Total) [µL]	Pressure [kPa]	Time [s]	Volume (TL-channel) [µL]	Pressure [kPa]	
Ab(I)-Ag reaction	Analyte (CRP)	100	50	200	40 / 20	0.2 / 0.06	100 / 250	
Washing	Washing Buffer	100	150	250				
Ag-Ab(II) reaction	HRP	100	90	250	100	2.5 / 0.5	250	
Washing	Washing Buffer	100	300	250				
Enzymatic reaction	TMB	50	150	250	50 → 30	1.7 / 1.0	340 → 0	
Detection	TMB				10	0.3/0.1	340	
Recovery	Glycine Chloride	150	120	250	120	3 / 0.6	250	
Blocking	Washing Buffer	100	100	200	120	3 / 0.6	250	
Total time	700 + 450 = 1150s (19 min)							
Total volume	1.2mL including counter-flow							

Table 2. Target transport characteristics within our TL-ELISA sensors

Parameters		5.2 μm	2 μm
Width	W, μm	1000	
Sensor Length	L, μm	10.000	
Channel Length	L_{ch}, μm	21.000	
Height	H, μm	5.2	2
Injection time	t, s	20	35
Injected volume	V, nL	0.22	0.063
Size	$\lambda = L/H$	1900	5000
Antigen concentration	C_0, M	6.5×10^{-8}	
Number of injected molecules	$N = C_0 V$, mol	1.42×10^{-17}	0.41×10^{-17}
Volumetric flow	Q, μm³/s	10.9×10^6	2.0×10^6
Diffusivity	D, μm²/s	40	
Reaction kinetics, k_{on}	k_{on}, 1/Ms	1×10^6	
Reaction kinetics, k_{off}	k_{off}, 1/s	1×10^{-3}	
Reaction kinetics, K_D	$K_D = k_{off}/k_{on}$, 1/M	1×10^{-9}	
Binding site density	b_m, sites/μm²	100	
Damkohler number Da	$Da = k_{on} b_m L/D$	2.5×10^{10}	
Peclet Number Pe_s	$Pe_s = 6QL^2/DH^2W$	6.0×10^9	7.5×10^9
Depletion zone	$\delta = L Pe_s^{-1/3}$, μm	5.5	5.3
Flux function ($Pe_s \gg 1$)	$F \sim 0.81\, Pe_s^{1/3} + 0.71\, Pe_s^{1/6} - 0.2\, Pe_s^{-1/3}$	1465	1573
Collection rate	$J_D = D C_0 F/L$, mol/s	3.8×10^{-19}	4.0×10^{-19}
Collection time	N/J_D, s	37.2	10.3
Reaction equilibrium time	$t_r = (k_{off} + k_{on} C_0)^{-1}$, s	15.3	
Peclet Number Pe_h	$Pe_h = Q/DW$	273	45

Table 3. CRP analysis of standard samples of human serum L-consera I, II (operation parameters are the same as in Table 1)

TL-ELISA chip	Serum 3.7 µg/mL		Serum 20 µg/mL	
	Determined concentration ±1SD (%C.V.)	Recovery	Determined concentration ±1SD (%C.V.)	Recovery
5.2 µm	2.7±0.18 µg/mL (6.76%)	73%	16.8±1.16 µg/mL (6.93%)	84%
2 µm	2.9±0.22 µg/mL (7.78%)	78%	18.3±1.03 µg/mL (5.65%)	92%